

Original Article

Novel insight into the distribution of L-cells in the rat intestinal tract

Carl Frederik Hansen^{1,2}, Niels Vrang¹, Per Torp Sangild², Jacob Jelsing¹

¹Gubra Aps, Agern Alle 1, 2970 Hørsholm; ²Department of Human Nutrition, University of Copenhagen, Frederiksberg, Denmark

Received March 1, 2013; Accepted March 30, 2013; Epub April 19, 2013; Published April 30, 2013

Abstract: Background: Gut secreted incretin hormones and gastric bypass surgery currently provides some of the most successful treatments for diabetes and obesity respectively. However, despite the evident importance of the gut endocrine system no information exists on the total number and distribution of different types of endocrine cells in the gut. Here we have used the established preclinical Zucker Diabetic Fatty (ZDF) rat model which displays elevated levels of GLP-1 to assess L-cell distribution and L-cell dynamics in the full rostro-caudal extension of the rat intestinal tract. Methods: Using mathematically unbiased stereology we provide total and regional estimates of gut volume, gut surface area and the total number of L-cells throughout the intestinal tract in obese ZDF rats and lean controls. Results: The total number of L-cells in the lean and obese ZDF gut is estimated to 4.8 and 10.9 million, respectively, coupled with a corresponding near doubling in total gut volume and total surface area. L-cell numbers were found to be distributed rather evenly throughout the jejunum, ileum and colon. Conclusion: The present study provides the first stereological report of total L-cell number and L-cell distribution throughout the rat intestinal tract. In contrast to the currently held view, the majority of L-cells are actually located proximal to the traditionally defined ileum and colon.

Keywords: L-cell, GLP-1, diabetes, stereology, ZDF

Introduction

Along with the introduction of bariatric surgery as a treatment for obesity an increased scientific focus has been directed towards the endocrinology of the gut. Bariatric surgery results in significant weight loss and improvement in health and quality of life [1-3]. Furthermore, surgical procedures such as Roux-en-Y gastric bypass (RYGB) have proven effective in curing diabetes with reported remission rates of type 2 diabetes (T2D) up to 80% [4]. We know today that surgery leads to complex alterations in the secretion of a number of hormones involved in glucose and weight homeostasis (e.g. GIP, GLP-1, PYY, ghrelin and oxyntomodulin, for reviews see: [5, 6]) and that some of these hormones exert powerful effects on both appetite function and glucose homeostasis. A better understanding of the gut endocrine system in the normal and diseased gut is therefore pivotal in order to unlock the key to novel pharmacologi-

cal treatments of diabetes and other obesity-related syndromes.

The total size and length of the intestinal tract is an obstacle for accurate anatomical and quantitative assessments of specific cell populations in this organ. Hence, the vast majority of the anatomical knowledge about the gut endocrine system stems from studies examining distribution frequencies of specific endocrine cells at specific sites of the gut, rather than to actual total numbers of cells [5, 7-12]. The endocrine L-cell has attracted special attention over the past decades partly because of the powerful incretin effects of GLP-1 [13, 14]. However, the distribution and total numbers of L-cells throughout the intestinal tract remains unknown. Previous studies indicate that the density of L-cells in the gut epithelium increases from the duodenum to the rectum [8, 11, 15], which has led to the general view that the majority of L-cells are found in the distal part of

the gut [16-18]. This view is, however, challenged by several functional data demonstrating a rapid (within 15 minutes) increment in postprandial plasma GLP-1 levels [19-22] and a sustained GLP-1 release even in distally intestinal resected animals [20].

During the last decades, the introduction of design-based stereology, also known as unbiased stereology, has greatly improved the accuracy and reliability of quantification in biological research [23, 24]. The main strength of stereological methods is that it can account for three-dimensional structures in terms of three-dimensional quantities. This is in contrast to the two-dimensional sections which are often used for the observation. Thus, counting of cellular profiles and density measurements will inevitably lead to biased results if subtle changes in the size of cells or the reference organ are not accounted for. A number of stereological papers has been published on intestinal morphometry [25-28], however a detailed stereological analysis revealing the factual number of L-cells along the rostro-caudal extension of the gut has not yet been performed.

Materials and methods

Experimental animals

All animal experiments were conducted in accordance with internationally accepted principles for the care and use of laboratory animals, and in compliance with personal animal licenses (2008/561-1565) issued by the Danish Committee for Animal Research.

A total of ten homozygous (fa/fa) male Zucker diabetic fatty rats (ZDF) and ten lean ZDF (Fa/?) rats were obtained (Charles River, Germany) at the age of 9 weeks. The rats were housed under standard housing conditions (temperature $22 \pm 2^\circ\text{C}$, relative humidity $50 \pm 10\%$, light/dark cycle: 12/12, lights off at 16:00 PM) and with ad libitum access to Purina 5008 (Purina 5008, Charles River Germany) to induce programmed and consistent development of T2D. At 20 weeks of age (11 weeks on housing) rats were euthanized with CO_2 before decapitation. A 2 ml trunk blood sample was obtained to which was added 20 μl DPP-V inhibitor (Millipore catalogue no DPP4-010). Active GLP-1 was analyzed using an ELISA kit according to the manufacturer instructions (AKMGP-011, Shibayagi, Japan).

Histology

For each group, five randomly selected animals were processed for morphology. The entire intestinal tract was removed and immersion fixed and stored in 4% phosphate buffered formaldehyde until further processing. The intestinal tract was then subdivided into three anatomically distinct segments based on gross morphological markers: the duodenum from the pyloric sphincter to the duodenojejunal bend, the jejunioileum from the duodenojejunal bend to the caecum, and the colon from the caecum to the rectum. The ileum was not separated from the jejunioileum due to the lack of a clear gross morphological criterion. The length of each segment was measured. Each of the segments was embedded in a 4% agarose (60°C) and sampled systematically, uniform randomly into 4 mm slaps across the whole segment (**Figure 1A** and **1B**). Rendering a total of 24-30 slaps from each animal. Each slap was infiltrated overnight in paraffin, mounted 4 together in blocks of paraffin (Tissue-TEK III, Sakura, Denmark) and eventually cut into 5 μm thick paraffin sections on a Microm (HM340E, ThermoScientific, Denmark) (**Figure 1C**). Sections were mounted singly on separate object glasses, or pairwise as two consecutive sections (**Figure 1D**).

HE staining

One series of sections were stained with hematoxylin-eosin. Sections were de-paraffinized in toluene (Sigma-Aldrich, Denmark), rehydrated in degrading series of ethanol, stained in a Mayer's hematoxylin solution (MHS80, Sigma Aldrich, Denmark) and Eosin B solution (HT110280, Sigma-Aldrich), dehydrated and finally coverslipped (Pertex, Sakura, Denmark).

Immunohistochemistry

Series of neighboring sections were stained for GLP-2 immunoreactivity to visualize L-cells. Sections were de-paraffinized in toluene and rehydrated before antigen retrieval in citrate buffer (10 mM, pH 6, at 90°C) and blocking of endogenous peroxidase activity (in 1% H_2O_2). Sections were incubated with avidin and subsequently biotin (X0590, Dako, Denmark), blocked in swine serum and incubated overnight with the primary GLP-2 antibody diluted 1:32000 (the mouse GLP2-12F21-A7 antibody was kindly provided by Novo Nordisk A/S).

L-cell distribution in ZDF rats

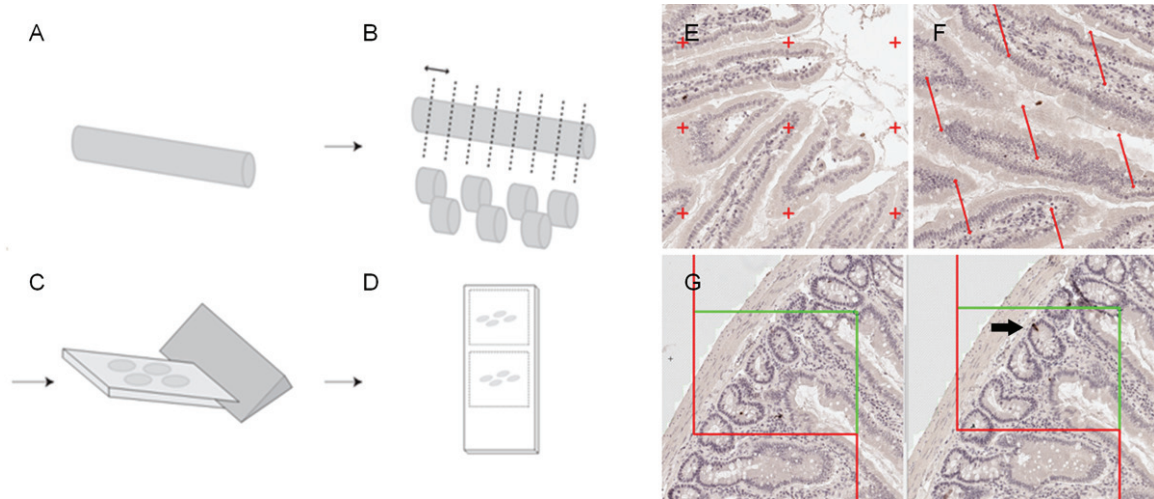


Figure 1. Tissue sampling and stereological probes. The intestinal tract was divided into the duodenum, jejunium and colon (A), embedded in agar and divided by systematically uniform random sampling into eight slabs (B). Each slab was embedded on their cut surface in paraffin and cut (C) into single or paired consecutive sections (D). Regional and specific cellular layer volume (i.e. the mucosa, submucosa and muscularis) was estimated by point counting (E). Surface area was estimated by counting intersections between line probes and the mucosal surface (F), and number was estimated using the physical disector on two paired neighbor sections (G). Arrow indicates the counting event where an immunoreactive cells is evident in one section and not the other.

On day 2, sections were rinsed in buffer, incubated for 30 min in biotin-coupled rabbit anti-mouse secondary antibody (1:2000), rinsed again and incubated in avidin-biotin complex (ABC, X0590, Dako) for 60 min. Following rinses, sections were incubated with biotinylated tyramine, re-incubated in ABC and developed in 0.04% diaminobenzidine. Sections were dehydrated and finally coverslipped (Pertex, Sakura).

Stereology

All stereological estimates were performed on digital slides scanned with a 20x objective on a Hamamatsu Nanozoomer 2.0 HT. Sections were evaluated in a random systematic way by use of the newCAST system (Visiopharm, Denmark).

Estimation of volume

Total gut volume and cellular layer volumes were estimated by point counting using a grid system where all points hitting the mucosa, submucosa and muscularis (including the serosa) cell layers were counted (**Figure 1E**). The number of points hitting the structure of interest was converted into volume according to:

$$Vol_{ref} = \sum_p * a(p) * t$$

Where $\sum P$ is the total number of points hitting the structure of interest, $A(p)$ is the area per

point and t is the distance in-between sections [23, 24].

Estimation of surface density and total epithelial surface area

Estimations of surface density (S_v) and surface area were performed by counting intersections between linear probes and the luminal side of the gut (**Figure 1F**) according to:

$$S_v = \frac{2 \cdot \sum I}{l_p \cdot \sum P}$$

Where $\sum I$ is the number of intersections of the test lines with the epithelium of the tunica mucosa, $l(p)$ is the test line length associated with a point of the grid and $\sum P$ is the number of test points falling on the reference volume [29]. Finally, the absolute surface area was estimated by multiplying the surface density with the reference volume. Estimates of surface density usually require isotropic or vertical sectioning protocols. However, due to the normal isotropic occurrence of villus (no preferred orientation of villus in 3D space) the present study was for all practical purposes performed on transverse sections only. The validity of these assumptions was tested beforehand (data not shown).

Estimation of the total number of L-cells

L-cells were identified using a specific GLP-2 antibody. GLP-1 and GLP-2 are both derived

from preproglucagon, and GLP-2 displays a perfect overlap with GLP-1 in L-cells [30]. The current antibody has previously been shown to colocalize 100% with GLP-1 in brainstem preproglucagon expressing neurons [31]. The total number of GLP-1/2 immunoreactive (ir) L-cells was estimated using the principle of the physical disector (**Figure 1G**) [29, 32, 33]. The method relies upon the principle that if a particle is seen in one section and not the previous, it is counted. For this purpose tissue sections were sampled as two consecutive levels and evaluated using 2D counting frames. The total number of L-cells in a defined sampling volume was counted and the particle density, N_v , was calculated as:

$$N_v = \Sigma Q / a_{(frame)} * h * \Sigma Q$$

Where $a_{(frame)}$ is the area per counting frame, h is the distance between the two sections, ΣQ is the total number of counted cells, and ΣP is the total number of points hitting the reference space. The total number of L-cells was finally determined by multiplying N_v with the total reference volume.

Correction for shrinkage

Whereas estimates of cell number are not influenced by tissue processing steps, all estimates of volume and surface area are biased by shrinkage. In order to correct for this and provide estimates of the absolute volume and surface area, we assessed the shrinkage coefficient for the rat gut in frozen and paraffin embedded sections sampled throughout the intestinal tract. The XY shrinkage (or in-section shrinkage) induced by dehydration and paraffin embedding was estimated by comparing point counts performed on frozen unshrunk sections with paraffin embedded sections. The Z shrinkage (or length shrinkage) was estimated by subjecting 2 cm long agarose embedded segments to dehydration before re-measuring the length. The surface shrinkage was estimated according to the procedures described by Karlsen and Pakkenberg [34].

Quantitative ISH

To estimate the total expression of preproglucagon (giving rise to GLP-1, GLP-2 and oxyntomodulin production in the endocrine L-cell) in situ hybridization was performed using a protocol described in detail previously [35, 36].

Preproglucagon mRNA was detected using P^{33} -labelled riboprobes directed against rat preproglucagon mRNA (bp 89–250; GenBank accession number: NM_012707). Sense RNA probes were used as negative controls. All sections were processed simultaneously and under the same conditions. Post-hybridization washes were performed at 62 and 67°C in 50% formamide. Following hybridization, the radioactively labeled sections were exposed to autoradiographic film and exposed for 8 hours. Images were acquired using the same camera and light settings in one session. Threshold setting and measurements were performed by an observer blinded to treatment. The same threshold settings were used for all images. Images were analyzed on a computerized image analysis system (NIH-image 1.62b). The total preproglucagon signal was quantified as the area of preproglucagon mRNA expression with a density above threshold by the mean pixel intensity per area multiplied with the sampling interval.

Stereological error and statistics

The precision of the estimator was evaluated in comparison to the biological variability in the sample. Mean regional coefficient of error (CE) was calculated using the approximation formula described by Gundersen and co-workers (1999) [24]. Using this formula, the mean estimated CE was 0.060 for regional volumes and 0.070 for regional numbers based on a mean number of 258 and 228 counting events, respectively, on 9 sections. The shape factor was estimated to 25 according to the nomogram by [23].

Results are presented as mean \pm SEM (standard error of the mean) unless otherwise stated. For all data statistical significance was tested using 2-way ANOVA with Bonferroni's post-test, except data on L-cell density in lean animals (2L) being tested using one-way ANOVA with Tukey's post-hoc test. $P < 0.05$ was considered statistically significant $P > 0.05$ is marked with *, $P > 0.01$ is marked with ** and $P > 0.001$ is marked ***. All statistics were performed using GraphPad Prism.

Results

In vivo results

At study start, the normoglycemic ZDF rats was approximately 25% heavier than the lean con-

L-cell distribution in ZDF rats

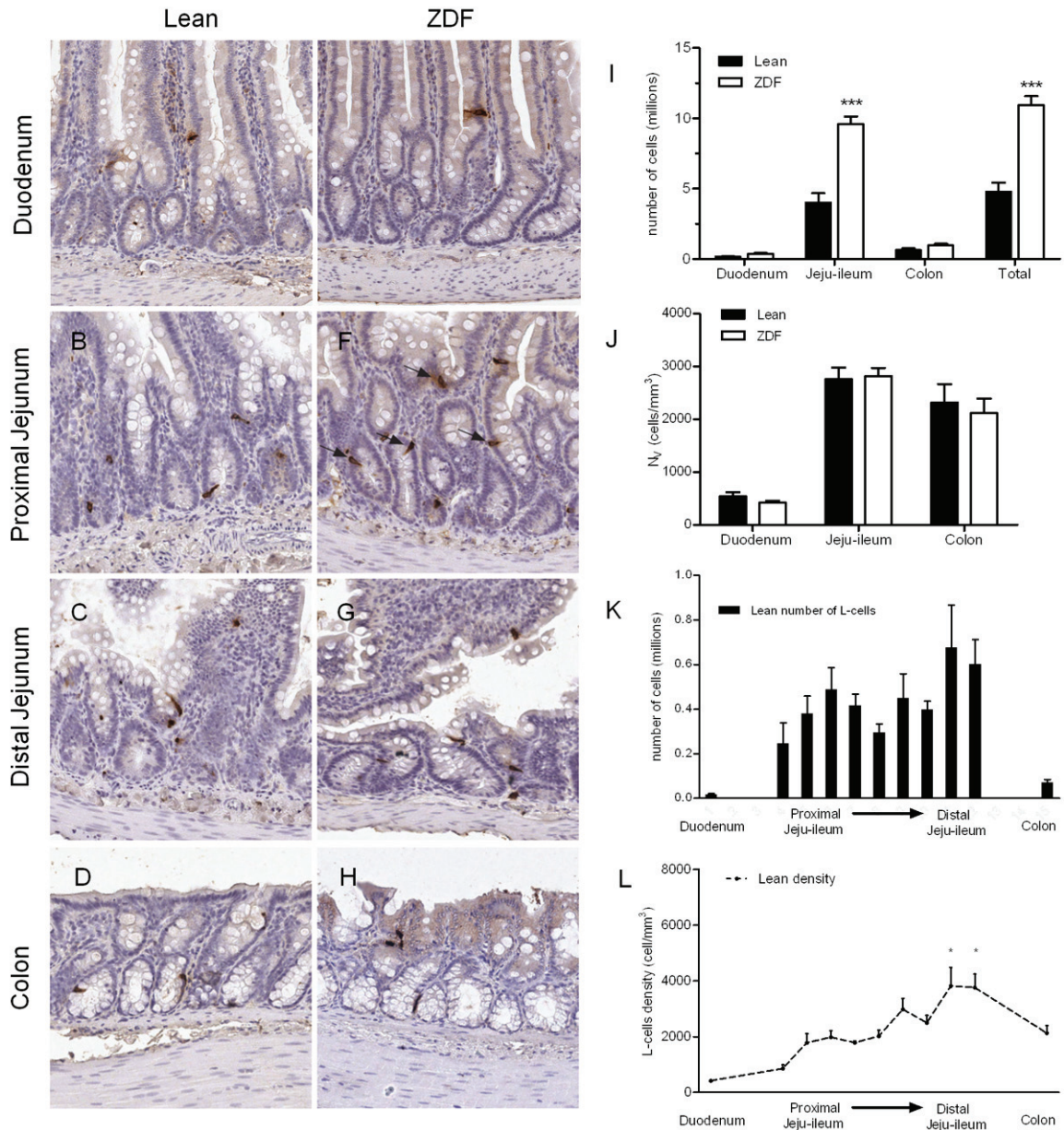


Figure 2. L-cell density and numbers. Representative images from duodenum (A, E) proximal (B, F) and distal (C-G) jejunoileum and colon (D-H) in lean and diabetic ZDF rats. L-cells are stained for GLP-2 immunoreactivity (arrows). Regional and total L-cell number (I) and density (J). L-cell number in throughout the gut of the jejunioileum and colon (K). L-cell density, displayed as line graph (L) with distal ileum tested significantly higher density than all other regions.

control group (ZDF 260 ± 9.2 ; lean 211 ± 3.5 g; $P < 0.0001$, $n = 10$). However, at the time of termination the body weight was no longer significantly different (ZDF 404 ± 7.84 ; Lean 386 ± 6.0 , $n = 10$) despite the food intake in obese ZDF rats being 2.7 fold higher than the lean control group (ZDF 37.6 ± 0.8 ; lean 14.0 ± 0.3 g; $P < 0.0001$). The reduced weight difference is a consequence of the onset and progression of diabetes as reflected in their terminal glucose

values (ZDF 26.4 ± 0.41 ; lean 5.5 ± 0.11 mmol/ml; $P < 0.0001$, $n = 10$). Similarly, terminal plasma levels of active GLP-1 were markedly increased in the ZDF group (ZDF: 19.7 ± 2.35 ; lean 10.6 ± 1.69 pg/mol; $P < 0.01$, $n = 10$).

L-cell number

The distribution and stereological estimation of L-cells in the rat gut is shown in **Figure 2**. GLP-2

L-cell distribution in ZDF rats

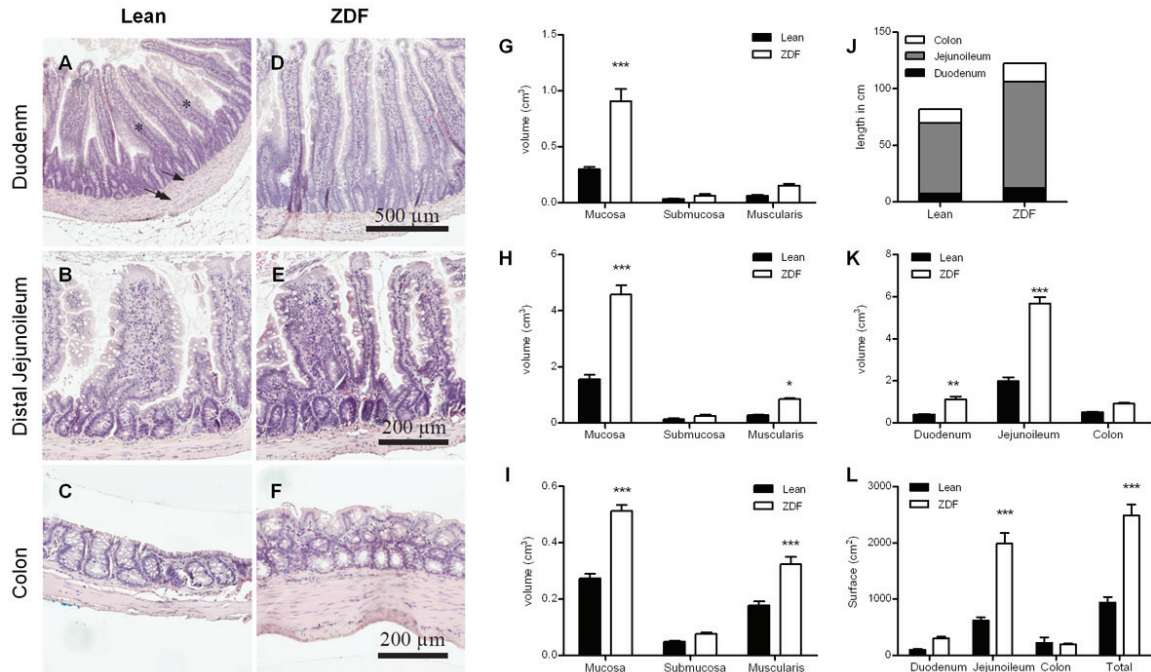


Figure 3. Volume of each of the cellular layers was quantified using stereological counting. Mucosa layer is marked with asterisk, submucosa by single arrow, and muscularis by double arrow. Representative images from duodenum (A, D), distal jejunum (B, E) and colon (C, F) in lean and diabetic ZDF rats counterstained with hematoxylin. Estimates of mucosa, submucosa and muscularis volumes in the duodenum (G), jejunum (H) and colon (I). Regional and total lengths of the intestinal segments (J) and stereological estimates of total regional volume (K). The total and regional intraluminal surface areas (L).

immunoreactive cells were easily identified by their classical bottle-like shape, minimal luminal contact and distribution intercalated between the epithelial cells in both crypts and villi (Figure 2A-H). The total number of L-cells was significantly higher in the diabetic ZDF rat (10.9 million, $P < 0.001$) and more than twice the level as compared to the lean ZDF rat (4.8 million) (Figure 2I). Interestingly, L-cells were predominantly confined to the jejunum accounting for more than 80% of the total L-cell pool (4.0 million and 9.6 million cells in the lean and obese ZDF respectively). In comparison, the number of L-cells in the colon was 0.63 million and 0.97 million in lean and ZDF rats, respectively. There was a tendency towards increased L-cell number in all gut segments, however, attaining statistical significance in the jejunum only (Figure 2I). By contrast, the mean density of L-cells was nearly identical in the jejunum (approximately 2800 cells/mm³) and colon (2200 cells/mm³), being markedly lower in the duodenum only (app. 500 cells/mm³) (Figure 2J). Distinguishing between proximal and distal gut is of course a matter of

definition. An analysis of L-cell number and density throughout the gut of lean ZDF rats revealed that nearly 60% of the total L-cell pool is confined proximal to the traditionally defined ileum (Figure 2K). The L-cell density, increases moderately throughout the extension of the jejunum being statistically significantly higher in the most caudal part of the small intestine, as compared to the proximal part ($P < 0.05$, Figure 2L).

Volume and surface area

All stereological sampling and staining procedures allowed for a clear differentiation of the specific cell layers and cell types (Figure 3A-F). In general, the duodenum was characterized by long, thin and straight villi, with an increased appearance of unattached mucosal structures in the jejunum (representing long villi cut in the transverse plane). The colon was characterized by short luminal villi and several goblet cells dispersed in the epithelium. The stereological analyses of gut volumes in the ZDF rat demonstrated marked changes in both regional and cellular layer volumes when compared to the

L-cell distribution in ZDF rats

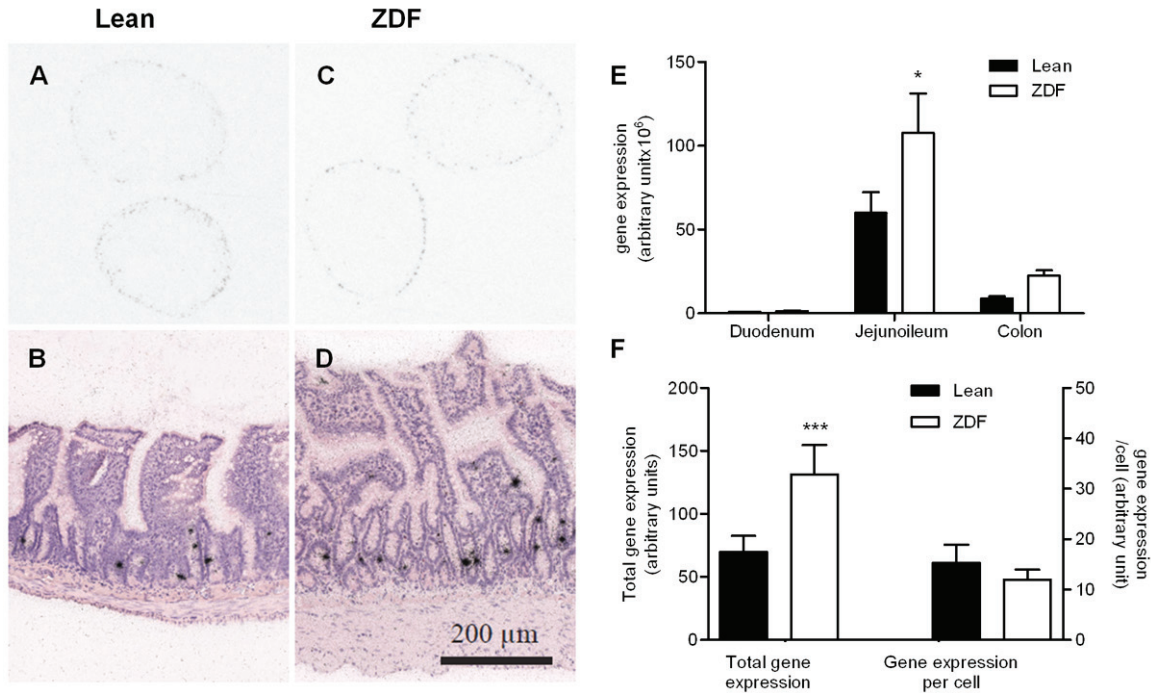


Figure 4. Gene expression analyses. Representative images of preproglucagon expression in the jejunioleum on autoradiographic film (A, C) and emulsion dipped sections (B, D). Regional total preproglucagon expression (E) and total gene expression (left axis) as well as expression per cell (right axis) (F).

lean phenotype (Figure 3G-I). The most pronounced expansion in the ZDF rat was seen in the mucosa cell layers in the duodenum (Figure 3G), jejunioleum (Figure 3H) and colon (Figure 3I). The expansion of cellular volume was also evident in the muscularis layers, being statistically significant in all regions except for the duodenum (Figure 3G-I). Although terminal body weight was similar in lean and diabetic ZDF rats, total gut length was 50% longer in diabetic ZDF rats (Figure 3J). Total regional volume was also markedly increased in ZDF rats (Figure 3K). The increased mucosal volume was accompanied by a similar increase in mucosal surface area, the only exception being the colon (Figure 3L). All estimates are provided as absolute values corrected for shrinkage with a mean volume correction factor of 47% and a linear surface shrinkage of 34%.

Preproglucagon expression

The majority of preproglucagon mRNA-expression was confined to jejunioleum with an apparent similar expression density between both groups (Figure 4A and 4C). Individual L-cells was identified on emulsion dipped sections, in a pattern similar to the immunohistochemical

stainings. (Figure 4B and 4D). In accordance with the immunohistochemical data on L-cell number, quantification of preproglucagon mRNA was found predominantly in the jejunioleum (approximately 85% of total mRNA) and colon (approximately 15%), with almost no expression in the duodenum (Figure 4E). The semi-quantitative in situ hybridization revealed a significant and almost 100% increase in total preproglucagon expression in the ZDF group compared to the lean controls (Figure 4F). However, when taking the number of L-cells into consideration the relative preproglucagon mRNA expression per cell (total preproglucagon expression divided by total L-cell number) was similar between phenotypes (Figure 4F).

Discussion

The present study provides the first stereological report of total L-cell number and L-cell distribution throughout the rat intestinal tract. We demonstrate that in the normal rat gut the total number of L-cells is approximately 4.8 million. In comparison, the normal rat pancreas contains an estimated total of 3.2 million insulin producing beta-cells highlighting the enormous size of the gut endocrine system relative to

other endocrine organs [37]. Furthermore, our data underscores the plasticity of the gut by the observation that diabetic ZDF rats exhibited more than doubling of total gut volume and L-cell number compared to lean controls. L-cell density, however, is unchanged between the two phenotypes indicating that signals triggering increased epithelial proliferation will lead to quantitatively similar relative increases in the number of endocrine cells. L-cell density in the different regions of the intestinal tract appears to be genetically determined.

Traditionally, the ileum and terminal colon have been identified as the primary localization for the L-cell population, being that in animal [7, 11, 38, 39] or man [18, 40]. This general assumption has led several L-cell studies to specifically focus on the distal ileum and colon [7, 9, 11, 12, 41]. Consequently, only few studies have included samples throughout the different gut segments [10, 15, 42]. These studies examine L-cell densities, and found that the distal part of the intestine holds the greatest cell density. However, counts of cellular profiles and reports of cell densities [11, 12, 43] do not take into consideration the potential massive contribution from gut hypertrophy leading to potential incorrect conclusions regarding L-cell distribution and number. In contrast to the general view, our quantitative data demonstrate that L-cell numbers are distributed along the full rostrocaudal extent of the jejunoileum with an increase in L-cell density in the distal part of this segment only. The rostral part of the jejunoileum contains almost as many GLP-2 immunoreactive cells as the distal gut. Along with the increase in L-cell number we observed a significant increase in total preproglucagon mRNA expression and plasma GLP-1 concentrations, whereas preproglucagon expression per cell was unaffected. Thus, even though mRNA expression does not necessarily reflect corresponding peptide levels our data indicate that the marked increase in plasma GLP-1 level as seen in the ZDF animals is related to the increased number of L-cells, rather than an increase transcriptional activity per cell.

Increased preproglucagon mRNA expression, as well as increased GLP-1 immunoreactive tissue content has previously been reported in the ZDF rat [43]. Irrespective of diabetic status, preproglucagon expression was shown to be

confined mainly to the large intestine, and highly elevated in obese, hyperglycemic animals [43]. A potential influence of disrupted leptin receptor signaling on L-cell dynamics has also been indicated in the large intestine of db/db mice, including increases in length, mucosa thickness and number of L-cells compared to non-diabetic controls [15]. There are several indications of functional leptin receptor activity in the gut, including leptin receptor expression on intestinal L-cells, in both rodent and man [44]. Peripheral administrations of leptin stimulate GLP-1 secretion in rats and *ob/ob* mice [44, 45] and enhance anorexia and weight loss induced by native GLP-1 or GLP-1 agonist. It is possible that the absence of functional leptin receptors may be associated with increased L-cell mRNA expression possibly as a compensatory homeostatic mechanism. However, the marked changes in total L-cell number may also be related to the differences in food intake and/or high levels of circulating glucose. Oral nutrients such as glucose and fat are known to stimulate GLP-1 secretion from the endoluminal side [46, 47]. High constant levels of circulating glucose in the diabetic ZDF rat could also potentially affect GLP-1 secretion and cell turnover. Interestingly, non-digestible carbohydrates have also been shown to promote L-cell differentiation in the colon (39) indicating that the hyperphagia in the ZDF rat may potentially be triggering gut hypertrophy per se. The increased total surface area in the duodenum and jejunoileum leads to an increased nutrient-absorbing area and nutrient-stimulated area. The possibility that food changes can drive gut hypertrophy is supported by reports on increased villus length and increased cell number in mice fed a high-fat diet for 8 weeks [48]. Moreover, previously published data in rodent models of gastric surgery [49, 50] also demonstrate a marked mucosal hypertrophy and increased number of L-cell in the regions of the gut exposed to partly undigested food components further substantiates this hypothesis. In this respect, it should be noted that both gastric bypass models were normoglycemic pre- and post-surgery, indicating that glycemic changes are likely not the main contributor, although a role of glucose in the control of L-cell number cannot be excluded. Finally, it should be noted that GLP-2, which is synthesized and secreted from the L-cells in a 1:1 stoichiometric ratio with GLP-1 [30], is a potent intestinal

L-cell distribution in ZDF rats

growth factor and inhibitor of apoptosis [51-53]. The increase in L-cell number and total preproglucagon expression leading to enhanced GLP-2 secretion could tentatively provide a positive feedback mechanism to further stimulate gut hypertrophy.

Most available data on gut hypertrophy is based on qualitative criteria [54] or by measuring indirect parameters such as villus height and crypt depth [55, 56]. Even though villus height and crypt depth may be used to identify major morphological changes in the intestinal tract [57, 58], this procedure can be hampered by the diverse ramification of intestinal villus and the concurrent changes in gut length which is often not corrected for. So far, there have only been a limited number of studies describing this very complicated organ in a systematic quantitative manner [25-28]. In this respect, it is worth emphasizing that the mean epithelial volume in the small intestine (duodenum and jejunoleum) of the rat previously has been shown to be in the range of 2500 mm³ with a surface area of 500-700 cm² [59]. These data corresponds well to the quantitative estimates presented herein, underscoring the validity of the stereological methods. Moreover, it should be recognized that the quantitative gene expression levels presented herein are estimated as total mRNA expression in series of sections throughout the gut hereby taking into account the marked increase in gut volume and L-cell number. This is in contrast to standard quantitative PCR data being normalized and presented as levels per mg tissue hereby obscuring potential changes related to differences in total volume.

Despite the obvious benefits and validity of the stereological sampling and the data presented herein, one should take into considered potential limitations. First of all, L-cells were identified by GLP-2 immunohistochemistry. Even though GLP-1 immunoreactive cells have been shown to overlap with GLP-2 [30] we cannot conclude that GLP-2 immunohistochemistry labels all L-cells in the gut. Immunohistochemical labeling procedures may vary from laboratory to laboratory based on antigenicity and labeling techniques. Moreover, recent data indicates that enteroendocrine cells may have a much broader potential for expression of multiple peptide precursors than is generally believed [60, 61]. Thus, the classical view on specific

endocrine lineages (i.e. distinct L, K, I cell lineages) may be changing [62].

In a translational point of view, our data may provide an explanation for the rapid increment in plasma GLP-1 levels observed after ingesting glucose or mixed meals, and before nutrients have entered the presumed L-cell rich distal intestinal regions [19-22]. Resection of the distal small intestine or colectomy do not lead to changes in GLP-1 release after an oral glucose load in man [20]. This suggests that the GLP-1 immediately secreted following glucose ingestion mainly stems from upper gut L-cells and not from distal cells in the ileum, colon and rectum. The present findings may also be central for understanding the mechanisms involved in the dramatic changes in glucose homeostasis following gastric bypass surgery. Surgical procedures such as Roux-en-Y gastric bypass (RYGB) leads to a rapid (usually within days) resolution of diabetes in more than 80% of obese patients with T2D [1, 4, 63] which is temporally associated with massive increases in plasma GLP-1 and PYY levels [64-66]. The rapid elevation in plasma GLP-1 and PYY levels may be related to the rapid delivery of undigested nutrients to the upper small intestine stimulating the large rostral L-cell population.

In conclusion, using stereological methods we demonstrate that L-cells in the rat intestine are distributed rather evenly throughout the jejunoleum to the distal colon. This is in contrast to the general belief that L-cells are confined to the distal ileum and colon, but in good agreement with a number of functional data. Moreover, increased plasma GLP-1 levels in the obese ZDF rat are associated with an increased number of L-cells in the intestinal tract and greatly increased gut volume, as well as increased total preproglucagon mRNA levels. The L-cell density, however, is unaffected which provides support for the hypothesis that the endocrine cell pool is genetically encoded in the various gut segments and that signals leading to increased epithelial proliferation will cause similar adaptive quantitative effects on L-cell numbers.

Acknowledgements

Funding: This research was supported by the Danish Agency for Science, Technology and Innovation by a personal stipend to CFH.

Declaration of interest

FH, NV and JJ are currently employed by Gubra. PTS has nothing to declare.

Address correspondence to: Jacob Jelsing, Gubra ApS, Agern Alle 1, 2970 Hørsholm, Denmark. Phone: (+45) 31522652; E-mail: jacob@gubra.dk

References

- [1] Sjoström L. Bariatric surgery and reduction in morbidity and mortality: experiences from the SOS study. *Int J Obes (Lond)* 2008; 32 Suppl 7: S93-97.
- [2] Pories WJ, Swanson MS, MacDonald KG, Long SB, Morris PG, Brown BM, Barakat HA, deRamon RA, Israel G, Dolezal JM and et al. Who would have thought it? An operation proves to be the most effective therapy for adult-onset diabetes mellitus. *Ann Surg* 1995; 222: 339-350; discussion 350-352.
- [3] Kim S and Richards WO. Long-term follow-up of the metabolic profiles in obese patients with type 2 diabetes mellitus after Roux-en-Y gastric bypass. *Ann Surg* 2010; 251: 1049-1055.
- [4] Buchwald H, Estok R, Fahrback K, Banel D, Jensen MD, Pories WJ, Bantle JP and Sledge I. Weight and type 2 diabetes after bariatric surgery: systematic review and meta-analysis. *Am J Med* 2009; 122: 248-256, e245.
- [5] Tharakan G, Tan T and Bloom S. Emerging therapies in the treatment of 'diabesity': beyond GLP-1. *Trends Pharmacol Sci* 2011; 32: 8-15.
- [6] Rhee NA, Vilsboll T and Knop FK. Current evidence for a role of GLP-1 in Roux-en-Y gastric bypass-induced remission of type 2 diabetes. *Diabetes Obes Metab* 2012; 14: 291-298.
- [7] Bryant MG and Bloom SR. Distribution of the gut hormones in the primate intestinal tract. *Gut* 1979; 20: 653-659.
- [8] Evans GS and Potten CS. The distribution of endocrine cells along the mouse intestine: a quantitative immunocytochemical study. *Virchows Arch B Cell Pathol Incl Mol Pathol* 1988; 56: 191-199.
- [9] Barbosa AJ, Nogueira JC, Penna FJ and Polak JM. Distribution of enteroglucagon- and polypeptide YY-immunoreactive cells in the gastrointestinal tract of the white-belly opossum (*Didelphis albiventris*). *Histochemistry* 1987; 88: 37-40.
- [10] Mortensen K, Christensen LL, Holst JJ and Orskov C. GLP-1 and GIP are colocalized in a subset of endocrine cells in the small intestine. *Regul Pept* 2003; 114: 189-196.
- [11] Eissele R, Goke R, Willemer S, Harthus HP, Vermeer H, Arnold R and Goke B. Glucagon-like peptide-1 cells in the gastrointestinal tract and pancreas of rat, pig and man. *Eur J Clin Invest* 1992; 22: 283-291.
- [12] Grigoryan M, Kedees MH, Charron MJ, Guz Y and Teitelman G. Regulation of Mouse Intestinal L Cell Progenitors Proliferation by the Glucagon Family of Peptides. *Endocrinology* 2012 Jul; 153: 3076-88.
- [13] Holst JJ. The physiology of glucagon-like peptide 1. *Physiol Rev* 2007; 87: 1409-1439.
- [14] Drucker DJ. The biology of incretin hormones. *Cell Metab* 2006; 3: 153-165.
- [15] Pinto HC, Portela-Gomes GM, Grimelius L, Kohnert KD, de Sousa JC and Albuquerque MA. The distribution of endocrine cell types of the gastrointestinal mucosa in genetically diabetic (db/db) mice. *Gastroenterology* 1995; 108: 967-974.
- [16] Rocca AS and Brubaker PL. Role of the vagus nerve in mediating proximal nutrient-induced glucagon-like peptide-1 secretion. *Endocrinology* 1999; 140: 1687-1694.
- [17] Nauck MA, Vardarli I, Deacon CF, Holst JJ and Meier JJ. Secretion of glucagon-like peptide-1 (GLP-1) in type 2 diabetes: what is up, what is down? *Diabetologia* 2011; 54: 10-18.
- [18] Varndell IM, Bishop AE, Sikri KL, Uttenthal LO, Bloom SR and Polak JM. Localization of glucagon-like peptide (GLP) immunoreactants in human gut and pancreas using light and electron microscopic immunocytochemistry. *J Histochem Cytochem* 1985; 33: 1080-1086.
- [19] Balks HJ, Holst JJ, von zur Muhlen A and Brabant G. Rapid oscillations in plasma glucagon-like peptide-1 (GLP-1) in humans: cholinergic control of GLP-1 secretion via muscarinic receptors. *J Clin Endocrinol Metab* 1997; 82: 786-790.
- [20] Nauck MA, Siemsgluss J, Orskov C and Holst JJ. Release of glucagon-like peptide 1 (GLP-1 [7-36 amide]), gastric inhibitory polypeptide (GIP) and insulin in response to oral glucose after upper and lower intestinal resections. *Z Gastroenterol* 1996; 34: 159-166.
- [21] Herrmann C, Goke R, Richter G, Fehmann HC, Arnold R and Goke B. Glucagon-like peptide-1 and glucose-dependent insulin-releasing polypeptide plasma levels in response to nutrients. *Digestion* 1995; 56: 117-126.
- [22] Ghatei MA, Uttenthal LO, Christofides ND, Bryant MG and Bloom SR. Molecular forms of human enteroglucagon in tissue and plasma: plasma responses to nutrient stimuli in health and in disorders of the upper gastrointestinal tract. *J Clin Endocrinol Metab* 1983; 57: 488-495.
- [23] Gundersen HJ and Jensen EB. The efficiency of systematic sampling in stereology and its prediction. *J Microsc* 1987; 147: 229-263.

L-cell distribution in ZDF rats

- [24] Gundersen HJ, Jensen EB, Kieu K and Nielsen J. The efficiency of systematic sampling in stereology—reconsidered. *J Microsc* 1999; 193: 199-211.
- [25] Van Ginneken C, Van Meir F and Weyns A. Stereologic characteristics of pig small intestine during normal development. *Dig Dis Sci* 2002; 47: 868-878.
- [26] Mayhew TM, Elbrond VS, Dantzer V, Skadhauge E and Moller O. Structural and enzymatic studies on the plasma membrane domains and sodium pump enzymes of absorptive epithelial cells in the avian lower intestine. *Cell Tissue Res* 1992; 270: 577-585.
- [27] Mayhew TM. Geometric model of the rat intestinal mucosa for stereological evaluation of villus amplification factors. *J Microsc* 1984; 135: 337-346.
- [28] Mikkelsen HB, Larsen JO, Froh P and Nguyen TH. Quantitative Assessment of Macrophages in the Muscularis Externa of Mouse Intestines. *Anat Rec (Hoboken)* 2011; Epub ahead of print.
- [29] Pakkenberg B and Gundersen HJ. Total number of neurons and glial cells in human brain nuclei estimated by the disector and the fractionator. *J Microsc* 1988; 150: 1-20.
- [30] Orskov C, Holst JJ, Knuhtsen S, Baldissera FG, Poulsen SS and Nielsen OV. Glucagon-like peptides GLP-1 and GLP-2, predicted products of the glucagon gene, are secreted separately from pig small intestine but not pancreas. *Endocrinology* 1986; 119: 1467-1475.
- [31] Vrang N, Hansen M, Larsen PJ and Tang-Christensen M. Characterization of brainstem preproglucagon projections to the paraventricular and dorsomedial hypothalamic nuclei. *Brain Res* 2007; 1149: 118-126.
- [32] Sterio DC. The unbiased estimation of number and sizes of arbitrary particles using the disector. *J Microsc* 1984; 134: 127-136.
- [33] Gundersen HJ, Bagger P, Bendtsen TF, Evans SM, Korbo L, Marcussen N, Moller A, Nielsen K, Nyengaard JR, Pakkenberg B and et al. The new stereological tools: disector, fractionator, nucleator and point sampled intercepts and their use in pathological research and diagnosis. *APMIS* 1988; 96: 857-881.
- [34] Karlsen AS and Pakkenberg B. Total numbers of neurons and glial cells in cortex and basal ganglia of aged brains with Down syndrome—a stereological study. *Cereb Cortex* 2011; 21: 2519-2524.
- [35] Kristensen P, Eriksen J and Dano K. Localization of urokinase-type plasminogen activator messenger RNA in the normal mouse by in situ hybridization. *J Histochem Cytochem* 1991; 39: 341-349.
- [36] Vrang N, Larsen PJ, Jensen PB, Lykkegaard K, Artmann A, Larsen LK and Tang-Christensen M. Upregulation of the brainstem preproglucagon system in the obese Zucker rat. *Brain Res* 2008; 1187: 116-124.
- [37] Bock T, Svenstrup K, Pakkenberg B and Buschard K. Unbiased estimation of total beta-cell number and mean beta-cell volume in rodent pancreas. *APMIS* 1999; 107: 791-799.
- [38] Polak JM, Bloom S, Coulling I and Pearse AG. Immunofluorescent localization of enteroglucagon cells in the gastrointestinal tract of the dog. *Gut* 1971; 12: 311-318.
- [39] Yamada J, Tauchi M, Rerkamnuaychoke W, Endo H, Chungsamarnyart N, Kimura J, Kurohmaru M, Hondo E, Kitamura N, Nishida T and Hayashi Y. Immunohistochemical survey of the gut endocrine cells in the common tree shrew (*Tupaia belangeri*). *J Vet Med Sci* 1999; 61: 761-767.
- [40] O'Brien RM and Granner DK. Regulation of gene expression by insulin. *Physiol Rev* 1996; 76: 1109-1161.
- [41] Cani PD, Hoste S, Guiot Y and Delzenne NM. Dietary non-digestible carbohydrates promote L-cell differentiation in the proximal colon of rats. *Br J Nutr* 2007; 98: 32-37.
- [42] Van Ginneken C, Verlinden K, Van Meir F, Sys S and Weyns A. A stereologic evaluation of glucagon-like peptide-1 (GLP-1) mucosal cells in the small intestine of the developing pig. *Anat Embryol (Berl)* 2002; 205: 153-157.
- [43] Berghofer P, Peterson RG, Schneider K, Fehmann HC and Goke B. Incretin hormone expression in the gut of diabetic mice and rats. *Metabolism* 1997; 46: 261-267.
- [44] Anini Y and Brubaker PL. Role of leptin in the regulation of glucagon-like peptide-1 secretion. *Diabetes* 2003; 52: 252-259.
- [45] Williams DL, Baskin DG and Schwartz MW. Leptin regulation of the anorexic response to glucagon-like peptide-1 receptor stimulation. *Diabetes* 2006; 55: 3387-3393.
- [46] Elliott RM, Morgan LM, Tredger JA, Deacon S, Wright J and Marks V. Glucagon-like peptide-1 (7-36)amide and glucose-dependent insulinotropic polypeptide secretion in response to nutrient ingestion in man: acute post-prandial and 24-h secretion patterns. *J Endocrinol* 1993; 138: 159-166.
- [47] Roberge JN and Brubaker PL. Regulation of intestinal proglucagon-derived peptide secretion by glucose-dependent insulinotropic peptide in a novel enteroendocrine loop. *Endocrinology* 1993; 133: 233-240.
- [48] de Wit NJ, Bosch-Vermeulen H, de Groot PJ, Hooiveld GJ, Bromhaar MM, Jansen J, Muller M and van der Meer R. The role of the small intes-

L-cell distribution in ZDF rats

- tine in the development of dietary fat-induced obesity and insulin resistance in C57BL/6J mice. *BMC Med Genomics* 2008; 1: 14.
- [49] Cummings BP, Strader AD, Stanhope KL, Graham JL, Lee J, Raybould HE, Baskin DG and Havel PJ. Ileal interposition surgery improves glucose and lipid metabolism and delays diabetes onset in the UCD-T2DM rat. *Gastroenterology* 2010; 138: 2437-2446, e2431.
- [50] Bueter M, Lowenstein C, Olbers T, Wang M, Cluny NL, Bloom SR, Sharkey KA, Lutz TA and le Roux CW. Gastric bypass increases energy expenditure in rats. *Gastroenterology* 2010; 138: 1845-1853.
- [51] Brubaker PL, Izzo A, Hill M and Drucker DJ. Intestinal function in mice with small bowel growth induced by glucagon-like peptide-2. *Am J Physiol* 1997; 272: E1050-1058.
- [52] Drucker DJ, Erlich P, Asa SL and Brubaker PL. Induction of intestinal epithelial proliferation by glucagon-like peptide 2. *Proc Natl Acad Sci U S A* 1996; 93: 7911-7916.
- [53] Litvak DA, Hellmich MR, Evers BM, Banker NA and Townsend CM Jr. Glucagon-like peptide 2 is a potent growth factor for small intestine and colon. *J Gastrointest Surg* 1998; 2: 146-150.
- [54] Jin X, Zimmers TA, Zhang Z, Pierce RH and Koniaris LG. Interleukin-6 is an important in vivo inhibitor of intestinal epithelial cell death in mice. *Gut* 2010; 59: 186-196.
- [55] Viguera RM, Rojas-Castaneda J, Hernandez R, Reyes G and Alvarez C. Histological characteristics of the intestinal mucosa of the rat during the first year of life. *Lab Anim* 1999; 33: 393-400.
- [56] Bertoni S and Gabella G. Hypertrophy of mucosa and serosa in the obstructed intestine of rats. *J Anat* 2001; 199: 725-734.
- [57] Stearns AT, Balakrishnan A and Tavakkolizadeh A. Impact of Roux-en-Y gastric bypass surgery on rat intestinal glucose transport. *Am J Physiol Gastrointest Liver Physiol* 2009; 297: G950-957.
- [58] Sukhotnik I, Shamir R, Bashenko Y, Mogilner JG, Chemodanov E, Shaoul R, Coran AG and Shehadeh N. Effect of oral insulin on diabetes-induced intestinal mucosal growth in rats. *Dig Dis Sci* 2011; 56: 2566-2574.
- [59] Mayhew TM and Middleton C. Crypts, villi and microvilli in the small intestine of the rat. A stereological study of their variability within and between animals. *J Anat* 1985; 141: 1-17.
- [60] Habib AM, Richards P, Cairns LS, Rogers GJ, Bannon CA, Parker HE, Morley TC, Yeo GS, Reimann F and Gribble FM. Overlap of endocrine hormone expression in the mouse intestine revealed by transcriptional profiling and flow cytometry. *Endocrinology* 2012; 153: 3054-3065.
- [61] Egerod KL, Engelstoft MS, Grunddal KV, Nohr MK, Secher A, Sakata I, Pedersen J, Windelov JA, Fuchtbauer EM, Olsen J, Sundler F, Christensen JP, Wierup N, Olsen JV, Holst JJ, Zigman JM, Poulsen SS and Schwartz TW. A major lineage of enteroendocrine cells coexpress CCK, secretin, GIP, GLP-1, PYY, and neurotensin but not somatostatin. *Endocrinology* 2012; 153: 5782-5795.
- [62] Gribble FM. The gut endocrine system as a coordinator of postprandial nutrient homeostasis. *Proc Nutr Soc* 2012; 71: 456-462.
- [63] Schauer PR, Burguera B, Ikramuddin S, Cottam D, Gourash W, Hamad G, Eid GM, Mattar S, Ramanathan R, Barinas-Mitchel E, Rao RH, Kuller L and Kelley D. Effect of laparoscopic Roux-en-Y gastric bypass on type 2 diabetes mellitus. *Ann Surg* 2003; 238: 467-484; discussion 484-485.
- [64] le Roux CW, Aylwin SJ, Batterham RL, Borg CM, Coyle F, Prasad V, Shurey S, Ghatei MA, Patel AG and Bloom SR. Gut hormone profiles following bariatric surgery favor an anorectic state, facilitate weight loss, and improve metabolic parameters. *Ann Surg* 2006; 243: 108-114.
- [65] Korner J, Bessler M, Cirilo LJ, Conwell IM, Daud A, Restuccia NL and Wardlaw SL. Effects of Roux-en-Y gastric bypass surgery on fasting and postprandial concentrations of plasma ghrelin, peptide YY, and insulin. *J Clin Endocrinol Metab* 2005; 90: 359-365.
- [66] Vincent RP and le Roux CW. Changes in gut hormones after bariatric surgery. *Clin Endocrinol (Oxf)* 2008; 69: 173-179.